J. Geophys. 41, 111–122, 1975

Acoustic Normal Modes Generated by Explosive Sources

H.-H. Essen, H.-W. Kebe, J. Siebert

Institut für Geophysik, Universität Hamburg

Received May 30, 1974; Revised Version September 10, 1974

Abstract. The theory of normal modes is applied to sound-propagation data from a shallow-water area of the North Sea. The signals generated by explosives have been recorded by a vertical array of hydrophones. In order to resolve the different modes the time series are filtered by narrow bandpass filters. In general, observed propagation velocities and vertical amplitude distributions are in good agreement with values computed from a simple wave-guide model consisting of a liquid layer (water) above a liquid halfspace (sediments). However, observed amplitudes of higher modes are smaller than predicted by theory, which probably is due to mode-dependent reflection and scattering losses at the boundaries. An observed splitting of wave groups seems to be caused by bubbles.

Key words: Acoustic Normal Modes — Propagation Velocities — Vertical Amplitude Functions.

1. *Introduction*

In order to study the interaction of underwater sound with random oceanographic wave fields simultaneous measurements are planned in an experimental site westward of the island of Sylt in the North Sea. Acoustic investigations using explosive and CW (continuous wave) sources have been started.

For acoustic propagation within a shallow water area the most important perturbations result from the boundaries, especially from surface waves. Surface waves have been studied intensively at the Sylt site along a profile with different wave recorders yielding both the wave heights and the directional distributions (Hasselmann *et al.*, 1973). When proceeding from the assumption that acoustic and surface wavelengths are of the same order, the interaction processes can be described by the theory of resonant wave-wave interaction (Essen and Hasselmann, 1970). According to this theory the attenuation of the direct signal as well as the distribution of the scattered field may be computed.

In this paper only acoustic measurements are presented. The underwater sound is generated by explosive sources. A vertical array of eight hydrophones is used in order to resolve the structure of the acoustic wave

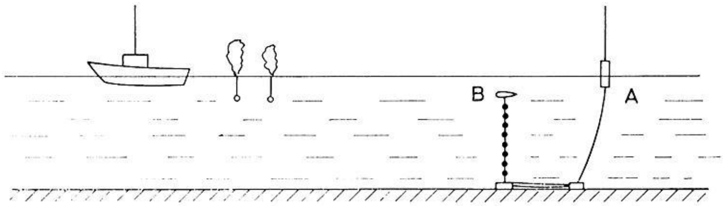

Fig. 1. Experimental configuration (schematic): A = Telemetry buoy, B = Vertical array of eight hydrophones

field, which in the case of shallow water is given by a superposition of discrete modes. The purpose of this experiment is to verify an acoustic waveguide model for the Sylt site.

Normal-mode investigations in shallow water areas were made by various authors. It turned out that the two-layered fluid model, first treated by Pekeris (1948), yields good agreement between theory and measurements. Kind (1970) worked with explosives and analysed the seismogram of one hydrophone by narrow bandpass filters and found the mode group velocities. Tolstoy (1958) used a CW source and compared the measured and theoretically-predicted horizontal structure of the acoustic pressure field. The group velocities as well as the vertical amplitude functions of the different modes were experimentally determined by Ferris (1972). Short pulses were produced by a CW source (400 and 750 cps) and recorded by a vertical array of hydrophones.

The measurements presented in this paper differ from those of Ferris (1972) with respect to the acoustic source and the analysed frequencies (50–300 cps). These low frequencies are of interest in the theory of acoustic-surface wave interaction.

2. *Method of Measurements*

Experiments with explosive sources were carried out during a test cruise with the vessel "Uthörn" at the Sylt site in December 1972. The method of measurements is illustrated in Fig. 1 (Kebe, 1973). The telemetry buoy (*A*) on the surface is moored and connected to a vertical chain of eight hydrophones (*B*) by cable. This cable is also part of the mooring system and connects the hydrophones with an eight-channel FM-FM-Multiplex-Equipment inside the telemetry buoy. A streamlined subsurface floatation element maintains the hydrophone chain in the vertical position. This position of the hydrophone array is verified by the simultaneous onset times of the signals at all hydrophones (cf. Fig. 3). The received FM-Multiplex-signal from the telemetry buoy is recorded on tape. The signal is also demodulated and simultaneously recorded on strip charts.

The explosion points were located at intervals of 300—500 m along a profile of 6.3 km in length. Separate detonations were made with exploders and bursting charges of various types.

3. Theoretical Wave-Guide Model

Sound propagation in shallow water is best represented by normal modes. Shallow implies here that the depth of water is of the order of a few acoustic wavelengths. The normal modes are free wave solutions of a layered halfspace, with the ocean as the uppermost layer. It is assumed that the sound velocity increases with depth. Due to the resulting angle of total reflection at the layer boundaries only a finite (frequency-dependent) number of modes is trapped within the overlying layers. The different modes are characterised by their propagation velocities and amplitude dependence on depth.

For distances r much larger than the water depth h_1 the acoustic pressure generated by a point source ($r=0$, $x_3=d$) can be described by a Fourier integral (Pekeris, 1948),

$$p(t, r, x_3) = r^{-\frac{1}{2}} \int_0^{\infty} \sum_{n=1}^{N(\omega)} a_n(\omega)\, \varphi_n(d)\, \varphi_n(x_3) \cdot \exp\left(i\left(\omega t - k_n r + \frac{\pi}{4}\right)\right) d\omega \tag{1}$$

where $a_n(\omega)$ depends on the source characteristics and waveguide model, $\varphi_n(x_3)$ is a vertical amplitude function which is a solution of an eigenvalue problem, and k_n are eigenvalues given by a dispersion relation,

$$f_n(\omega, k_n) = 0 \tag{2}$$

The acoustic energy propagates with the group velocity,

$$v_n = \frac{d\omega}{dk_n} = -\frac{\partial f_n}{\partial k_n} \bigg/ \frac{\partial f_n}{\partial \omega} \tag{3}$$

Computed group velocities for different wave-guide models are shown as a function of frequency and mode number n in Fig. 2. The parameters of the sedimental layering are taken from former seismic refraction investigations (Essen *et al.*, 1973).

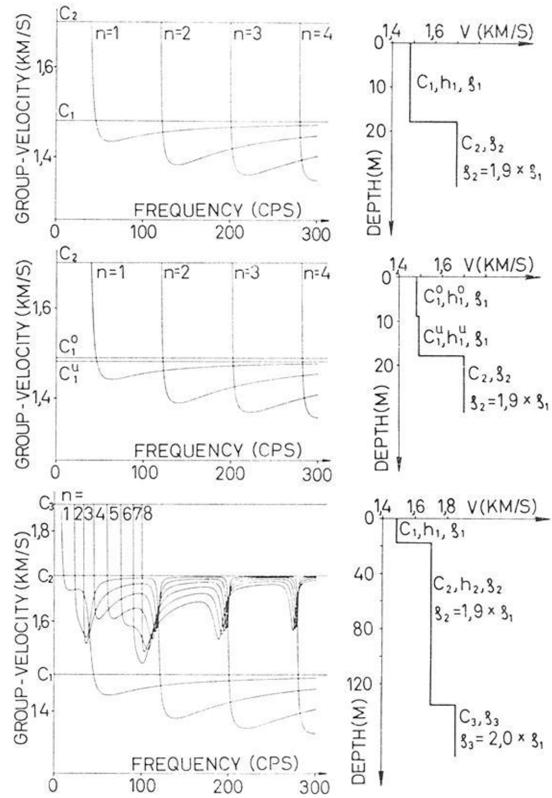

Fig. 2. Group velocities calculated as function of frequency and mode number (n) for different wave-guide models

c_i = sound velocity
h_i = thickness
ϱ_i = density
} of layer $i = 1, 2, 3$

The vertical sound-velocity profile of the water layer was not measured during the experiment but can be considered constant, because measurements made during the same season showed fluctuations of less than 1 ms^{-1} varying randomly with depth. This is due to homogeneous mixing by tides and waves during the winter months.

The first panel of Fig. 2 shows the group velocities of the simplest model, a water layer of constant sound velocity overlying a homogeneous sediment halfspace. The second model includes a weak discontinuity in the centre of the water layer. The resulting change of group velocities is negligible. (For higher frequencies and greater water depths the influence of discontinuities becomes more important. Ferris (1972) shows a case of a second-mode arrival before the first-mode arrival.) The third panel applies to a model with a two-layered sediment halfspace. The uppermost sediment layer thickness is 6.5 times the water depth (Essen *et al.*, 1973). The group velocities of modes trapped within both the water and sediment layer show a complicated dependence on frequency. However, for modes which are trapped in the water layer only, there is almost no influence of the sediment layering, as being expected.

Numerical computations were also made for a model with non-zero gradients of sound velocity of the water and sediment layer. The differences compared with the simplest model of Fig. 2 (first panel) were found to be small. In the following only this simple two-layer model is used.

In accordance with other authors (Pekeris, 1948; Kind, 1970; Ferris, 1972) shear waves in the sediment halfspace have been neglected. Possible shear-wave velocities are less than the sound velocity of water, and in consequence there are no trapped modes within the water layer. Only in the limit of small shear-wave velocities (some 100 ms^{-1}) does the approximation of normal modes become valid. From different methods shear-wave velocities of 100–500 ms^{-1} were measured in fully saturated sediments (Hamilton, 1971).

In the case of Fig. 2 (first panel) the following relations are found,

$$\varphi_n(x_3) = \sin\left(\sqrt{\frac{\omega^2}{c_1^2} - k_n^2} \cdot x_3\right) \tag{4}$$

(arbitrarily normalized)

$$f_n(\omega, k_n) = \sqrt{k_n^2 - \frac{\omega^2}{c_2^2}}\, \varphi_n(h_1) + \frac{\varrho_2}{\varrho_1}\, \varphi_n'(h_1) = 0 \tag{5}$$

$$a_n(\omega) = G(\omega)\sqrt{k_n}\left(\varphi_n(h_1)\,\frac{\partial f_n(\omega, k_n)}{\partial k_n}\right)^{-1} \tag{6}$$

where $G(\omega)$ depends on the frequency spectrum of the source only.

4. *Experimental Results*

During this test experiment acoustic signals from different charges were recorded along one vertical array of eight hydrophones at varying distances between the array and the explosion points. Explosive sources yield a broad frequency spectrum. Computed normal mode group velocities and vertical amplitude functions, however, are valid for fixed frequencies only. In order to resolve modes by travel times the received pressure signals have to be filtered by narrow bandpass filters designed from the following considerations:

For a fixed range r (= distance source-receiver) and a fixed frequency $\nu\left(\nu = \frac{\omega}{2\pi}\right)$ the time difference of the arrivals of wave groups of mode m and n is given by,

$$\tau_{nm} = \frac{r}{v_m} - \frac{r}{v_n} \tag{7}$$

where v_n, v_m are the respective group velocities, cf. (3).

The relation (7) applies in the theoretical limit of sharply defined frequencies. This is incompatible with a finite-duration signal, which is necessary for separation of modes by travel times. In order to obtain a finite pulse length Δt one has to consider a finite frequency interval $\Delta\nu$ determined by the uncertainty relation,

$$\Delta\nu \approx \frac{1}{\Delta t} \tag{8}$$

Therefore two conditions must be satisfied in order to resolve the modes by travel times. First,

$$\tau_{nm} > \Delta t \tag{9}$$

where τ_{nm} can be increased by increasing the distance r of sources and receiver, cf. (7), and secondly, the change of group velocity of an individual mode within the interval $\Delta\nu$ must be small compared with the difference between the group velocities v_n and v_m in the relation (7). This condition can be most easily satisfied by bandpass filters of bandwidth $\Delta\nu$ smaller than the frequency interval between two adjacent modes and centre frequencies approximately in the centres of these intervals. From the model of Fig. 2 (first panel) it is found,

$$\Delta\nu \lesssim 80 \text{ cps} \tag{10}$$

and:

central frequency (cps):	85	170	255
number of modes:	1	2	3

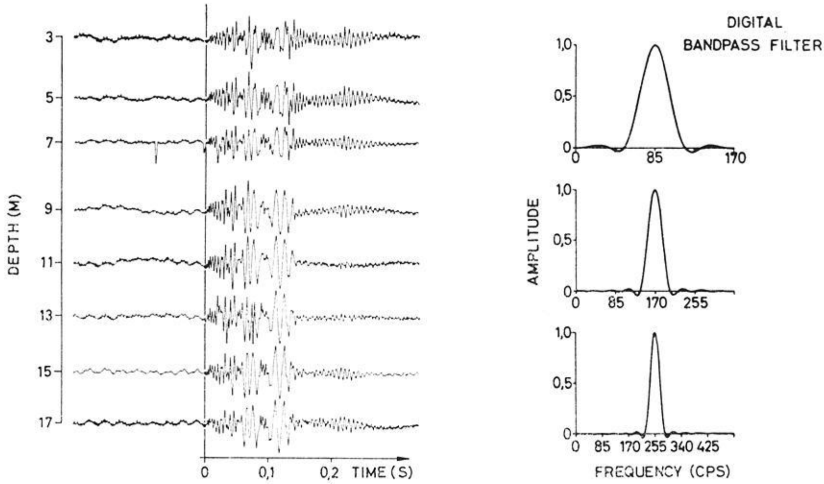

Fig. 3. Left: Original recordings of the vertical hydrophone array (normalized to same maximum amplitude); Right: Digital bandpass filter curves

Substituting (10) into (8), a requirement for the propagation distance r is obtained from condition (9) and the computed group velocities, cf. (7) and Fig. 2 (first panel):

$$r \gtrsim 1 \text{ km} \tag{11}$$

Modes simultaneously trapped within the water and at least one sediment layer can be neglected. Due to the depth of the first sediment layer (6.5 times the water depth) the energy density of those modes is small. As seen in Fig. 2 these modes propagate with velocities higher than the sound velocity of water (as opposed to modes trapped within the water layer only). In fact, no modes with velocities higher than the sound velocity of water were observed.

An original recording of the vertical hydrophone array is shown in the left panel of Fig. 3. The distance r from the source was 4.1 km and the water depth was nearly constant within the range of propagation ($h_1 = 18 \pm 0.5$ m). The positions of the hydrophones are marked on the ordinate scale. The zero point of the time scale coincides with the first signal onset.

The right panel of Fig. 3 shows the filter curves chosen to satisfy the conditions given above. Fig. 4 shows the filtered time series of the received pressure signals. The time scales are the same as in the original seismograms, but the signal amplitudes are normalized to have the same maximum amplitude. The vertical lines indicated by mode numbers n

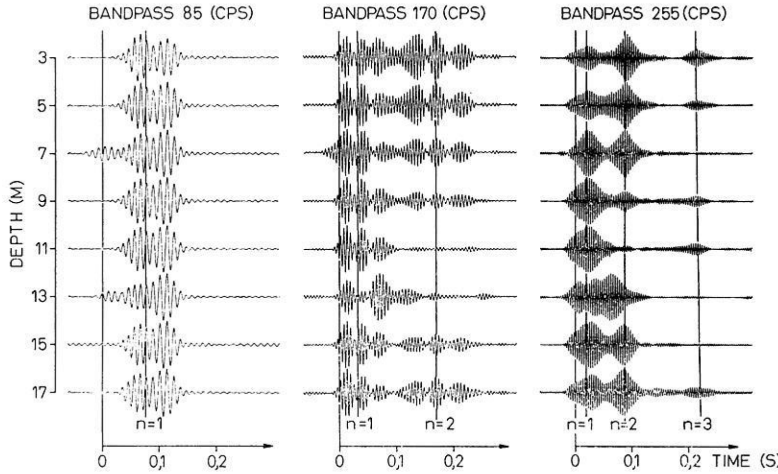

Fig. 4. Bandpass-filtered recordings at the central frequencies: 85, 170, 255 cps (normalized to same maximum amplitude)

mark the theoretical arrival times of the normal modes. They are computed from the group velocity curves of Fig. 2 (first panel) at the central frequencies of the bandpass filters. Because of the uncertainty relation the arrival times are not defined exactly but only within a limited interval. An additional broadening of this interval results from the variation of the group velocity within the frequency interval of the bandpass filters.

The single modes can be identified by their amplitude dependence on depth. In the case of the simplest two-layer model this is given by a sine-function, cf. (4). The number of nodes of this function in the water column is equal to the mode number n. The nodes are clearly identifiable in Fig. 4, as well as the phase reversal on either side of a node ($n = 2,3$). The positions of the nodes agree well with theoretical prediction. The observed and theoretical arrival times are also in good agreement. The "splitting" of wave groups belonging to one mode probably results from bubbles (see below). It should be mentioned that the signal of the hydrophone at 13 m depth obviously is disturbed.

Fig. 5 shows a more detailed analysis of the vertical amplitude function of the modes. The theoretical amplitudes are computed from the central frequencies, and it is assumed that they are nearly constant within the frequency interval of the bandpass filters, which is in fact fulfilled. The theoretical curves are matched to the measured points by the method of least squares. The depth dependence of the hydrophone sensitivity was corrected for this analysis.

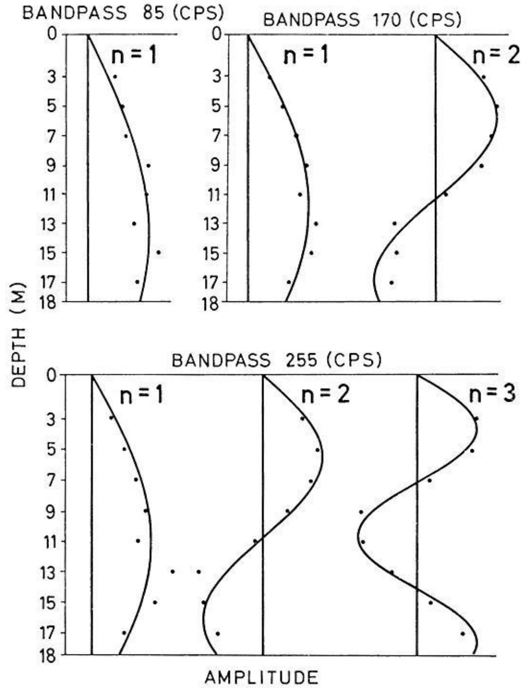

Fig. 5. Theoretical (lines) and observed (dots) vertical amplitude functions for various modes n (mode amplitude in arbitrary units)

Table 1. Comparison of observed and theoretical normal-mode amplitudes

Bandpass filter 170 (cps)	measured	theoretical
$\frac{\{a_n \varphi_n(d)\}\ n=2}{\{a_n \varphi_n(d)\}\ n=1}$	0.52	0.79

Bandpass filter 255 (cps)	measured	theoretical
$\frac{\{a_n \varphi_n(d)\}\ n=2}{\{a_n \varphi_n(d)\}\ n=1}$	0.95	1.1
$\frac{\{a_n \varphi_n(d)\}\ n=3}{\{a_n \varphi_n(d)\}\ n=2}$	0.22	0.44

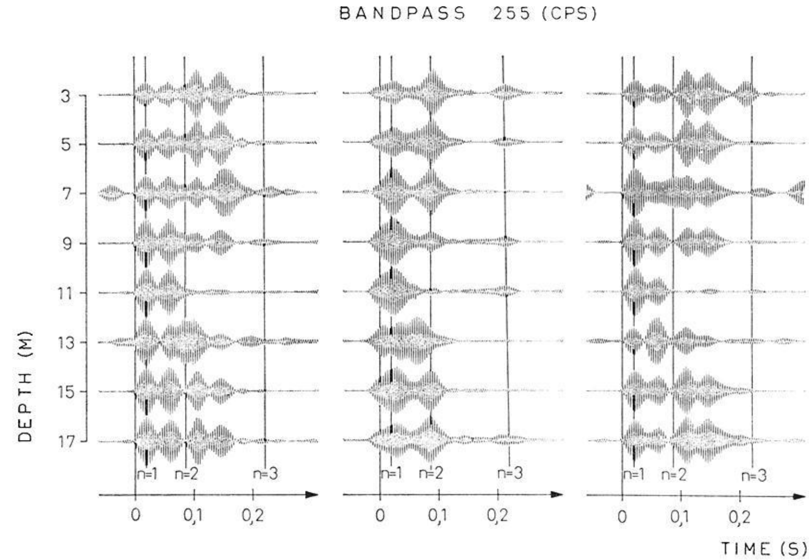

Fig. 6. Bandpass-filtered recordings for different charges (normalized to same maximum amplitude), from left to right: 1) bursting charge (cylindric, 15 g, mainly $Ba(NO_3)_2$), 2) exploder, 3) bursting charge (cubic, 27 g, mainly gun powder)

Relative maximum amplitudes of different modes at the same frequency are compared in Table 1. The theoretical values for a point source apply for the central frequencies of the bandpass filters. The charge depth was $d = 5$ m.

The measured amplitudes of the higher modes $n = 2,3$ are considerably smaller than expected from theory. Most probably this can be explained by the mode-dependent attenuation from reflection losses at the bottom (Ingenito, 1973) or scattering processes at the boundaries (Essen and Hasselmann, 1970).

Up to this point only results from one special explosion have been discussed. Fig. 6 shows three bandpass-filtered recordings from the same position of source and receiver, obtained, however, from different charges. The second column in Fig. 6 represents the recordings which have been discussed in detail above. The first and third column represent bandpass-filtered registrations, which are very similar but different from the second one. Thus, it is apparent that the main influence results from the brisance of the charges. Our interpretation is that the splitting of the wave groups belonging to the same mode is generated by bubbles. There are two reasons for this: The observed periods agree with those computed according to the formula of Willis (1951) and the periods are independent of the distance from the source (not shown in this paper).

The bursting charges mainly differ in two respects from the exploder: The travel times of the mode $n=2$ do not agree with the theoretical value, and the mode $n=3$ is not observed. Whereas the first effect probably results from an interference of first-mode bubbles with the second mode, the second effect is not yet understood. In spite of the divergence of the propagation velocities, the theoretical and measured vertical amplitude functions show nearly the same good agreement as in Fig. 5.

About 20 explosions have been analysed. Because of the bubbles, the smaller distances from the source, i.e. smaller than $r=4.1$ km, allow no clear separation of the modes. At distances greater than this value the signal was lost in the telemetry noise, so that all data shown in this paper were analysed for the one favourable shot distance of 4.1 km.

In spite of these experimental limitations, it is concluded that the measured data agree well with the theoretical values obtained from the simple two-fluid layer model.

Acknowledgements. Thanks are due to all our colleagues who helped in gathering the data. This work was supported by the Deutsche Forschungsgemeinschaft, Sonderforschungsbereich 94, Meeresforschung Hamburg.

References

Essen, H.-H., Hasselmann, K.: Scattering of low-frequency sound in the ocean, Z. Geophys. *36*, 655–678, 1970

Essen, H.-H., Hirschleber, H. B., Siebert, J.: Geschwindigkeits- und Dämpfungsmessungen an Sedimenten der Nordsee. Z. Geophys. *39*, 833–854, 1973

Ferris, R. H.: Comparison of measured and calculated normal-mode amplitude functions for acoustic waves in shallow water. J. Acoust. Soc. Am. *48*, 981–988, 1972

Hamilton, E. L.: Elastic Properties of Marine Sediments. J. Geophys. Res. *76*, 579–604, 1961

Hasselmann, K., Barnett, T. P., Bouws, E., Carlson, H., Cartwright, D. E. Enke, K., Ewing, J. A., Gienapp, H., Hasselmann, D. E., Kruseman, P., Meerburg, A., Müller, P., Olbers, D. J., Richter, K., Sell, W., Walden, H.: Measurements of Wind-Wave Growth and Swell Decay during the Joint North Sea Wave Project. Ergänzungsheft zur Dt. Hydrogr. Z. (8°) Nr. *12*, 1–95, 1973

Ingenito, F.: Measurements of mode attenuation coefficients in shallow water. J. Acoust. Soc. Am. *53*, 858–863, 1973

Kebe, H.-W.: Ein Meßverfahren zur Untersuchung von akustischen Streuprozessen im Flachwasser. Kongreßberichtswerk der Interocean, 849–860, 1973

Kind, R.: Auswertung seeseismischer Messungen mit einer digitalen Methode unter Anwendung der Theorie der Schallwellenausbreitung im Flachwasser. Z. Geophys. *36*, 549–567, 1970

Pekeris, C. L.: Theory of propagation of explosive sound in shallow water, Geol. Soc. Am. Mem. *27*, 43–70, 1948

Tolstoy, I.: Shallow water test of the theory of layered wave guides. J. Acoust. Soc. Am. *30*, 348–361, 1958
Willis, H. F.: Underwater explosions, time interval between successive explosions. British Report Wa-47-21, 1941

Dipl.-Phys. Heinz-Hermann Essen
Phys.-Ing. Hans-Werner Kebe
Dipl.-Phys. Jürgen Siebert
Institut für Geophysik der Universität
D-2000 Hamburg 13
Binderstraße 22
Federal Republic of Germany